

# Matching Accuracy Analysis of Fingerprint Templates Generated by Data Processing Method Using the Fractional Fourier Transform

Reiko Iwai, Hiroyuki Yoshimura

*Graduate School of Engineering, Chiba University, Chiba, Japan*

*E-mail: reiko@tu.chiba-u.ac.jp, yoshimura@faculty.chiba-u.jp*

*Received November 30, 2010; revised December 26, 2010; accepted December 30, 2010*

## Abstract

The matching accuracy of the fingerprint templates which were generated by our previously proposed data processing method using the fractional Fourier transform (FRT) was analyzed. The minimum error rate (MER) derived from the false acceptance rate (FAR) and the false rejection rate (FRR) is the criterion of the matching accuracy in this study, and was obtained statistically by the peak value of the normalized cross-correlation function between the fingerprint template and the intensity FRT of the subject's fingerprint. In our analysis, the fingerprint template was obtained as the intensity FRT of one-dimensional (1D) finite rectangular wave by which a line of a real fingerprint image is modeled. Moreover, various modified 1D finite rectangular waves were generated to derive the FAR. Furthermore, the 1D finite rectangular wave with random noise regarded as dirt of a fingerprint and the one with random vanishing ridges regarded as damage of a fingerprint were generated to derive the FRR. As a result, it was clarified that fingerprint templates generated by our data processing method using the FRT could provide high matching accuracy in the fingerprint authentication from the viewpoint of the MER.

**Keywords:** Fractional Fourier Transform, Fingerprint Authentication, Biometrics, Personal Information Protection

## 1. Introduction

In the previous study, we developed a new data processing method for generating the fingerprint template using the FRT [1-5] in order to take into account the protection of personal information [6]. In this study, we analyze the matching accuracy of the fingerprint templates generated by our previously proposed data processing method, because the biological identifier does not always have the same condition so that there is a possibility of false authentication. As the causes of the modification of the biological identifiers, especially for the fingerprint, sweat, sebum and dust, etc., can be considered. In general, the FAR and the FRR [7] are used as the criteria of the matching accuracy in the fingerprint authentication.

In the present study, in order to obtain the FAR and the FRR, the peak value of the normalized cross-correlation function between the fingerprint template and the intensity FRT of the subject's fingerprint image are

derived for various FRT's orders. The FRT's order is changed from 1.0 to 0.5 by 0.1. In particular, the FRT with the order of 1.0 is regarded as the conventional Fourier transform (FT). The small values of FRT's orders less than 0.5 are not considered, because we previously obtained the result that the most appropriate FRT's order is 0.9 [6]. In Section 2, the modeled authentic fingerprint image and its templates are indicated. In Section 3, the basic idea of the FAR, FRR and MER are explained and related to the analyses conducted in this study. In Section 4, by introducing the impostor fingerprint image, the behavior of the peak value of the normalized cross-correlation function between the fingerprint template and the intensity FRT of the impostor fingerprint image is analyzed. In Section 5, by introducing the modification of the authentic fingerprint image caused by dirt, small scar, etc., the behavior of the peak value of the normalized cross-correlation function between the fingerprint template and the intensity FRT of the authentic modified fingerprint image is also analyzed. In Section 6,

by use of the results obtained in Sections 4 and 5, the MER and the threshold in the fingerprint authentication are obtained for the FRT's orders from 1.0 to 0.5 by 0.1. Finally, in Section 7, conclusions in our study are described.

## 2. Fingerprint Template Corresponding to the FRT Intensity

### 2.1. Definition of the Fractional Fourier Transform (FRT)

The FRT is the generalization of a conventional FT. The FRT of 1D input data  $u(x)$  is defined [8,9] as

$$u_p(x_p) = \int u(x) \exp \left[ i\pi (x_p^2 + x^2) / s^2 \tan \phi \right] \times \exp \left[ -2i\pi x_p x / s^2 \sin \phi \right] dx, \quad (1)$$

where a constant factor has been dropped;  $\phi = p\pi/2$ , where  $p$  is the FRT's order;  $s$  is a constant. In particular, in the optical FRT,  $s$  is called a scale factor expressed in terms of  $s = \sqrt{\lambda f_s}$  where  $\lambda$  is the wavelength and  $f_s$  is an arbitrarily fixed focal length. In this paper, the value of  $s$  was fixed at 1.0. In particular,  $p$  takes a value of  $4n + 1$ ,  $n$  being any integer, the FRT corresponds to the conventional FT. The intensity distribution of the FRT (*i.e.*, the intensity FRT),  $I_p(x_p)$ , is obtained by calculating  $|u_p(x_p)|^2$ .

### 2.2. Relationship between a Modeled Authentic Fingerprint Image and the Template

We previously proposed a new data processing method to generate the fingerprint template by use of the FRT [6]. A finite rectangular wave shown in **Figure 1** was assumed to be the simplification of the authentic fingerprint image. In this paper, we enroll the fingerprint templates expressed in term of the intensity FRTs shown in **Figure 2**. The fingerprint templates were obtained from the application of Equation (1) to an authentic finite rectangular wave shown in **Figure 1** by changing the FRT's order. The intensity FRT of an authentic person's fingerprint image is called fingerprint template in this study. Matching between the template and the intensity FRT of newly scanned subject's fingerprint image is conducted in our analysis. The peak values of the intensity distributions in **Figures 2(a)** and **2(b)** are  $1.63 \times 10^7$  and  $4.34 \times 10^5$ , respectively. It is found from the comparison between **Figures 2(a)** and **2(b)** that the peak value of the intensity distribution falls remarkably and the width of spread increases when the value of the FRT's order  $p$  is 0.9. The cases of the other FRT's orders have also the

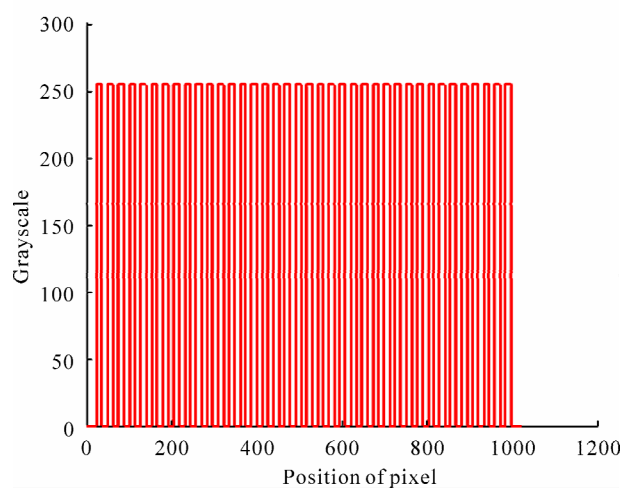
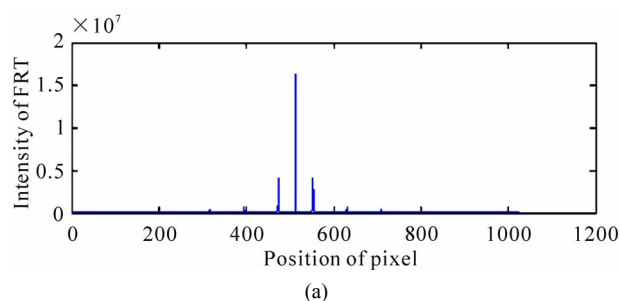
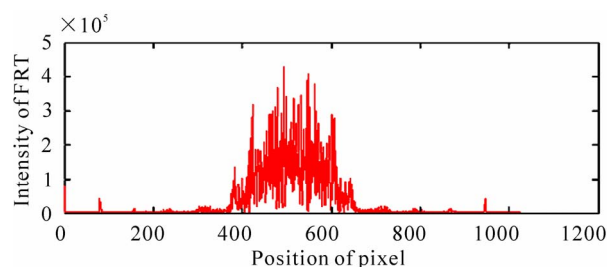


**Figure 1.** An authentic finite rectangular wave regarded as a modeled authentic fingerprint image.



(a)



(b)

**Figure 2.** Examples of the templates of an authentic finite rectangular wave shown in **Figure 1**, when  $ps =$  (a) 1.0 and (b) 0.9.

same tendency.

## 3. Matching Accuracy Analysis Based on the FAR, FRR and MER

**Figure 3** illustrates the basic concept of the FAR and the FRR. In the figure, the left-hand curve is the imposter distribution and the right-hand curve is the authentic distribution. The FAR is the probability of accepting impostors erroneously. As shown in the figure, it corresponds to an area of the impostor distribution higher than

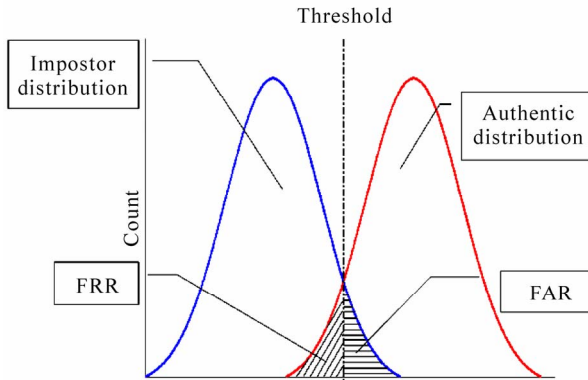


Figure 3. A basic concept of the FAR and the FRR.

the authentication threshold. On the other hand, the FRR is the probability of rejecting authentic person and corresponds to the area of the authentic distribution lower than the authentication threshold. The authentication threshold is decided by a value satisfied with the condition the FAR and FRR take the same value. It's called MER. In our analysis, the horizontal axis in **Figure 3** corresponds to the peak value of the 1D normalized cross-correlation function of the intensity FRTs for the two sets of fingerprint images.

In this paper, we prepare and analyze the authentic and impostor fingerprint images. First, a finite rectangular wave shown in **Figure 1** is regarded as modeling a line of authentic fingerprint image. Second, 100 kinds of the impostor finite rectangular waves are prepared to obtain the impostor distribution in **Figure 3**. Third, 100 kinds of the authentic finite rectangular waves which are superimposed by random noise (average  $\mu = 0$ , standard deviation  $\sigma = 12.75, 19.13, 25.50, 31.88, 38.25$ ) are prepared to obtain the authentic distribution in **Figure 3**. In addition, 100 kinds of the authentic finite rectangular waves with vanishing ridges (from 1 to 5 vanishing ridges at random positions) are prepared to obtain the authentic distribution. Finally, we derive the peak value of the cross-correlation function between the template of the authentic fingerprint image as shown in **Figure 2** and the intensity FRT of the impostor fingerprint image, or the one with dirt or small scar. Finally, we analyze the FAR and the FRR from the behavior of the peak value, and obtain the MER.

#### 4. Peak Value of the Normalized Cross-Correlation Function between the Fingerprint Template and the Intensity FRT of the Impostor Fingerprint

In order to derive the FAR, we prepared the intensity FARs of the impostor fingerprint images. The impostor

fingerprint images were made by changing the ridge's position randomly from the authentic finite rectangular wave shown in **Figure 1**. The authentic finite rectangular wave consisted of 1024 ( $2^{10}$ ) points. The number of ridges was 39 and the ridges were placed equally. One ridge consisted of 13 points and one groove also consisted of 13 points. On the other hand, in the impostor finite rectangular wave, one ridges also consisted of 13 points, but the positions of ridges were changed randomly between  $-10$  and  $10$  points from the ones in the authentic finite rectangular wave. **Figure 4** illustrates an example of the impostor finite rectangular wave regarded as the modeled impostor fingerprint image.

**Figure 5** shows the intensity FRTs of **Figure 4** when the FRT's orders  $ps = 1.0$  and  $0.9$ . The peak values of the intensity distributions in **Figures 5(a)** and **5(b)** are  $1.58 \times 10^7$  and  $5.56 \times 10^5$ , respectively. It is found from **Figure 5** that they have the same tendency as those of the authentic finite rectangular wave shown in **Figure 2**.

We quantitatively analyzed the behavior of the peak value of the normalized cross-correlation function between the authentic intensity FRT (*i.e.*, the fingerprint template) and the impostor intensity FRT. **Figure 6** illustrates an example of the normalized cross-correlation function between the fingerprint template shown in **Figure 2** and the intensity FRT shown in **Figure 5**. The peak values of the intensity distributions in **Figures 6(a)** and **6(b)** are 0.845 and 0.720, respectively. It is found from the comparison between **Figures 6(a)** and **6(b)** that the significant peak value is not seen and the width of spread increases when the value of the FRT's order  $p$  is 0.9.

**Figure 7** is the result showing the peak value of the normalized cross-correlation function between the fingerprint template and the impostor intensity FRT, when the FRT's order  $p$  is changed from 1.0 to 0.5 by 0.1. 100

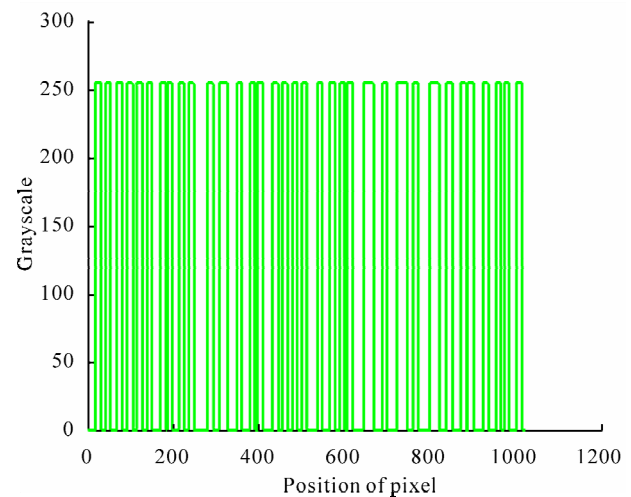
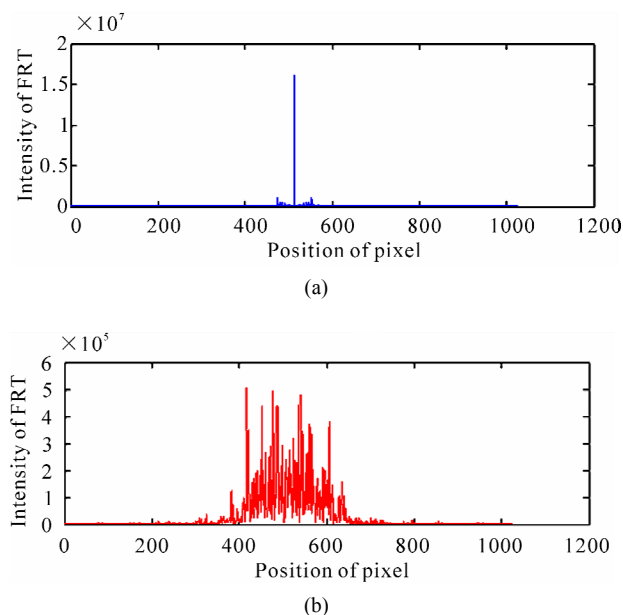
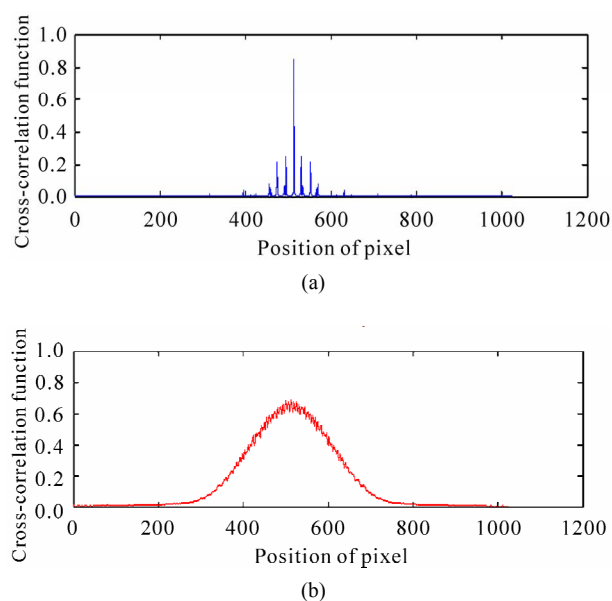


Figure 4. An example of the impostor finite rectangular wave regarded as modeled impostor fingerprint image.



**Figure 5.** Intensity FRT of the impostor finite rectangular wave shown in Figure 4, when  $ps =$  (a) 1.0 and (b) 0.9.



**Figure 6.** Normalized cross-correlation function between the fingerprint template shown in Figure 2 and the intensity FRT shown in Figure 5, when  $ps =$  (a) 1.0 and (b) 0.9.

kinds of impostor fingerprint images were used for each value of  $p$ . In **Figure 7**, the vertical and horizontal axes denote the peak value of the normalized cross-correlation function and the FRT's order, respectively. The symbols of circle in the figure denote the averaged values of the peak values. The error bars denote the standard deviations of the peak values and correspond to the width of spread of the impostor distribution shown in **Figure 3**.

We can understand from **Figure 7** that the peak values

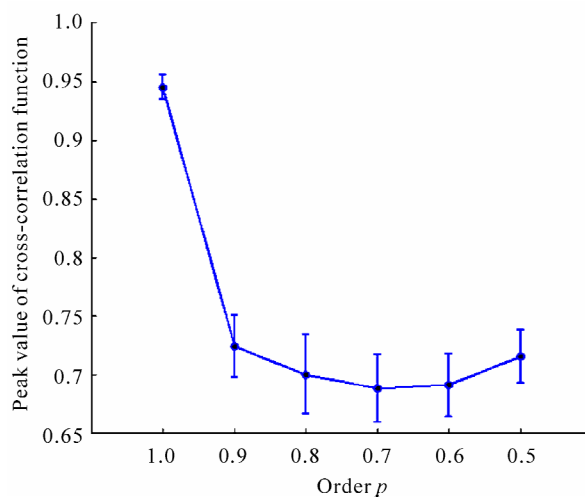


**Figure 7.** Behavior of the peak value of the normalized cross-correlation function between the fingerprint template and the intensity FRT of the impostor fingerprint image by changing the FRT's order.

of the normalized cross-correlation function are low when the non-integer FRT's orders are used. This fact means that the probability accepting impostors erroneously, *i.e.*, the FAR, would be low. As the reason why the FAR would be low in case of the non-integer FRT's orders, we can consider that the intensity FRTs with non-integer orders strongly includes the information on the impostor fingerprint image itself in comparison with the intensity FT (*i.e.*, the FRT intensity with the order of 1.0).

## 5. Peak Value of the Normalized Cross-Correlation Function between the Fingerprint Template and the Intensity FRT of the Modified Authentic Fingerprint

In order to derive the FRR, we considered the following two cases: 1) the case of adding random noise to the authentic finite rectangular wave such as dirt and sebum and 2) the case of vanishing ridges on the authentic finite rectangular wave such as small scar.

### 5.1. Case of Adding Random Noises

We considered the random noise characterized by the mean value  $\mu = 0$  and the normalized standard deviation  $\sigma_n = 0.05, 0.075, 0.1, 0.125$  or  $0.15$ . The normalized standard deviation  $\sigma_n$  indicates the standard deviation  $\sigma$  normalized by 255 corresponding to the maximum value of an authentic finite rectangular wave shown in **Figure 1**. In particular, the degree of the ran-

dom noise corresponds to a 1/3 value of height of the ridges at the most, when  $\sigma_n = 0.15$ . Therefore, we did not consider the random noise more than  $\sigma_n = 0.15$ . As an example, **Figure 8** denotes the authentic finite rectangular wave with random noise of  $\mu = 0$  and  $\sigma_n = 0.05$ . Then, the intensity FRT of **Figure 8** was obtained as shown in **Figure 9**, when the FRT's orders  $ps = 1.0$  and  $0.9$ . The peak values of the intensity distributions in **Figures 9(a)** and **9(b)** are  $1.63 \times 10^7$  and  $4.53 \times 10^5$ , respectively. It is understood from the comparison between **Figures 2** and **9** that there is little difference between the fingerprint template and the intensity FRT of the authen-

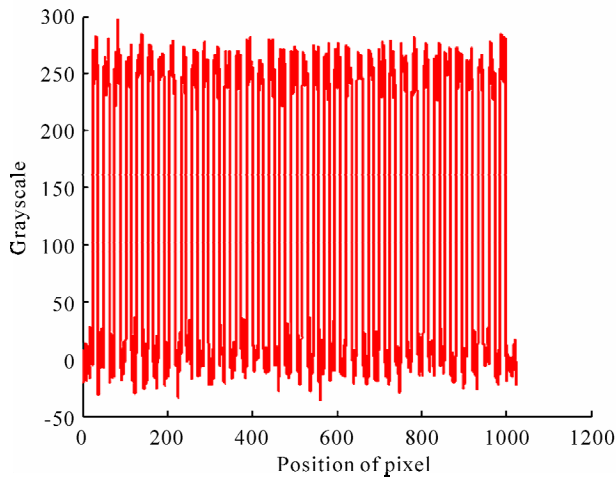


**Figure 8.** An example of the authentic finite rectangular wave with random noise, when  $\mu = 0$  and  $\sigma_n = 0.05$ .

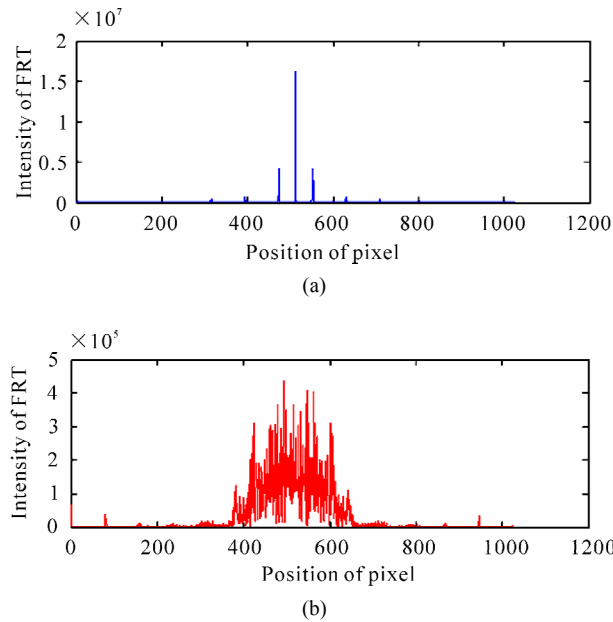


**Figure 9.** Intensity FRT of the authentic finite rectangular wave with noise shown in **Figure 8**, when  $ps =$  (a) 1.0 and (b) 0.9.

tic finite rectangular wave with random noise.

**Figure 10** shows an example of the normalized cross-correlation function between the fingerprint template shown in **Figure 2** and the intensity FRT shown in **Figure 9**. The peak values of the intensity distributions in **Figures 10(a)** and **10(b)** are 0.999 and 0.993, respectively. It is found from the comparison between **Figures 10(a)** and **10(b)** that the distribution has a projecting peak value and the width of spread increases when the value of the FRT's order  $p$  is 0.9.

**Figure 11** shows the behavior of the peak value of the normalized cross-correlation function between the fin-

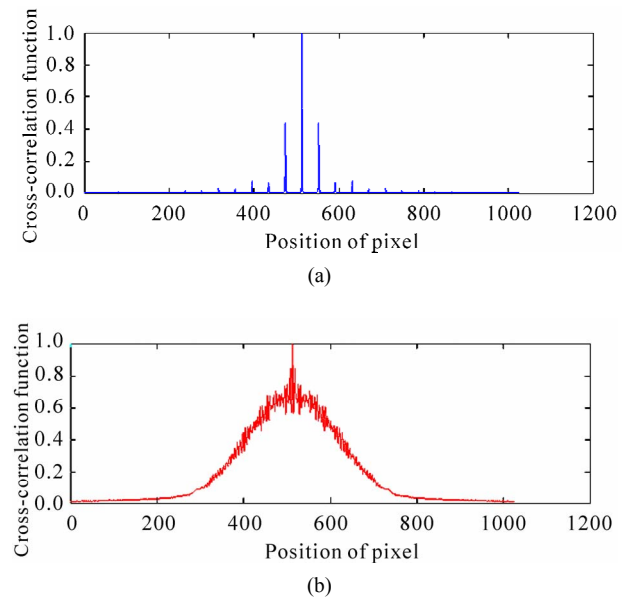


**Figure 10.** Normalized cross-correlation function between the fingerprint template shown in **Figure 2** and the intensity FRT shown in **Figure 9**, when  $ps =$  (a) 1.0 and (b) 0.9.

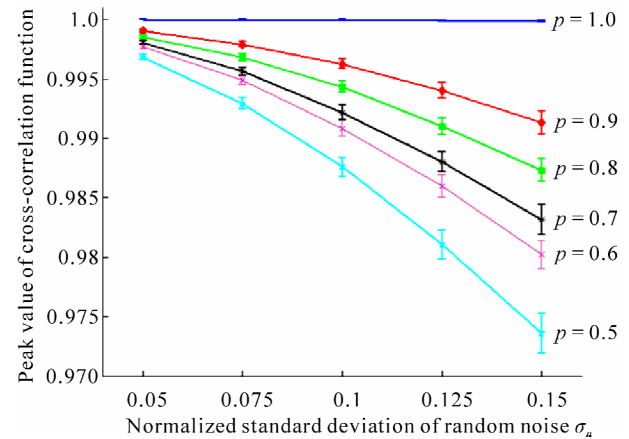


**Figure 11.** Behavior of the peak value of the normalized cross-correlation function between the fingerprint template and the intensity FRT of the authentic finite rectangular wave with random noise.

gerprint template and the intensity FRT of the authentic finite rectangular wave with random noise by changing the FRT's order from 1.0 to 0.5 by 0.1 and the normalized standard deviation of random noise  $\sigma_n$  from 0.05 to 0.15 by 0.025. The vertical and horizontal axes denote the peak value of the normalized cross-correlation function and the normalized standard deviation, respectively. The error bars denote the standard deviations of the peak values for 20 kinds of authentic finite rectangular waves with random noise having the same value of  $\sigma_n$ . Each curve corresponds to the result for each value of the FRT's order. The symbols of circle in the figure denote the averaged peak values.

We can understand from **Figure 11** that the matching accuracy judged as authentic person becomes worse with an increase in  $\sigma_n$  except the case of the FT ( $p = 1.0$ ) and with a decrease in the FRT's order  $p$ . As the reason, we can consider that the intensity FRTs are strongly affected by the degree of random noise and include the information on the random noise itself with a decrease in the FRT's order. However, the probability of rejecting authentic person erroneously is extremely low, because the peak values are nearly 1.0 for every FRT's order and normalized standard deviation of random noise. This fact means that the FRR would become very low.

## 5.2. Case of Vanishing Ridges

Next we analyzed the peak value of the normalized cross-correlation function between the fingerprint template and the intensity FRT of the authentic finite rectangular wave with vanishing ridges by changing the FRT's order from 1.0 to 0.5 by 0.1. We prepared 100 kinds of the authentic fingerprint images with 1 to 5 vanishing ridges at random positions. The more the number of vanishing ridges increases, the more the number of hurts increases. When the number of vanishing ridges is 5, 1/8 of the whole number of ridges is lost in the authentic fingerprint image. Therefore, we did not consider the number of ridges more than 6 to avoid further serious hurt. As an example, **Figure 12** shows an example of the authentic finite rectangular wave with five vanishing ridges at random positions. Then, the intensity FRT of **Figure 12** was obtained as shown in **Figure 13** when the FRT's orders  $ps = 1.0$  and 0.9. The peak values of the intensity distributions in **Figures 13(a)** and **13(b)** are  $1.24 \times 10^7$  and  $4.94 \times 10^5$ , respectively. It is understood from the comparison between **Figures 2** and **13** that there is little difference between the fingerprint templates and the intensity FRT of the authentic finite rectangular wave with vanishing ridges at random positions.

**Figure 14** shows an example of the normalized cross-correlation function between the fingerprint tem-

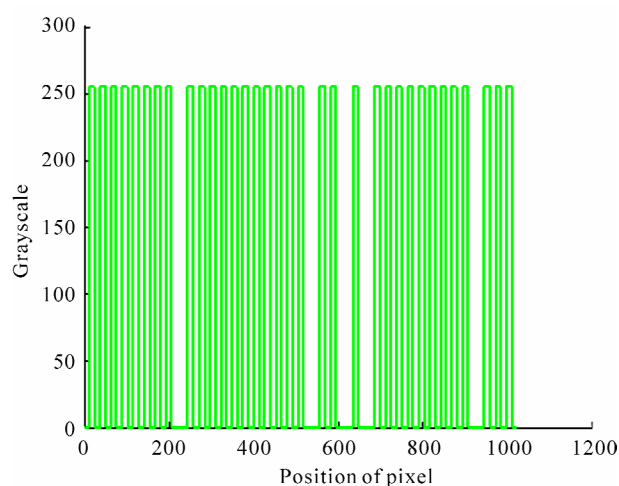
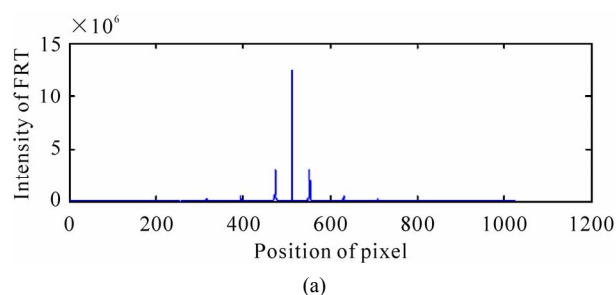
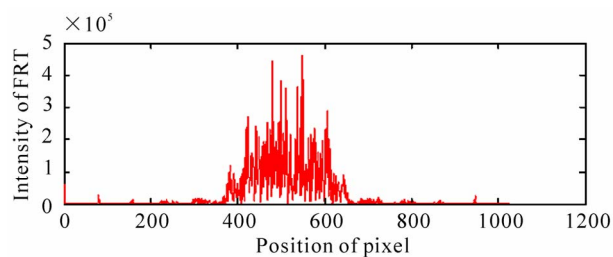


**Figure 12.** An example of the authentic finite rectangular wave with five vanishing ridges at random positions.



(a)



(b)

**Figure 13.** Intensity FRT of the authentic finite rectangular wave with five vanishing ridges at random positions shown in **Figure 12**, when  $ps =$  (a) 1.0 and (b) 0.9.

plate shown in **Figure 2** and the intensity FRT shown in **Figure 13**. The peak values of the intensity distributions in **Figures 14(a)** and **14(b)** are 0.999 and 0.936, respectively. It is found from the comparison between **Figures 14(a)** and **14(b)** that the distribution has a projecting peak value and the width of spread increases when the value of the FRT's order  $p$  is 0.9.

We analyzed the effect of the number of vanishing ridges on the peak value of the normalized cross-correlation function between the fingerprint template and the intensity FRT of the authentic finite rectangular wave with vanishing ridges by changing the FRT's order  $p$

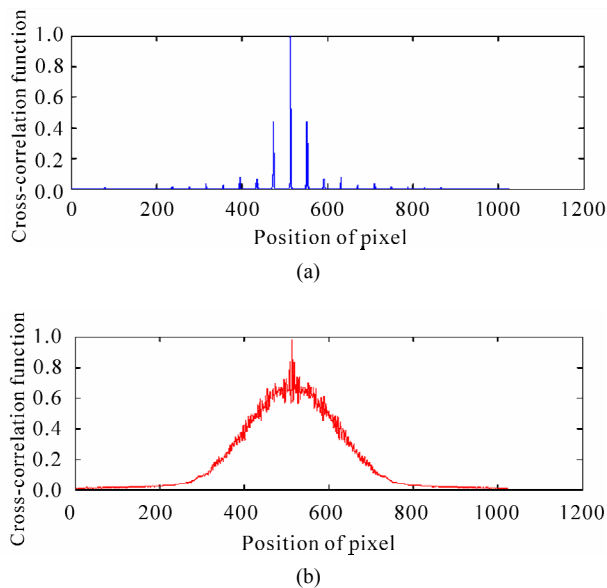


**Figure 14.** Normalized cross-correlation function between the fingerprint template shown in Figures 2 and the intensity FRT shown in Figure 13, when  $ps =$  (a) 1.0 and (b) 0.9.

from 1.0 to 0.5 by 0.1. **Figure 15** denotes the dependency of the peak value on the number of vanishing ridges and the FRT's order  $p$ . The vertical and horizontal axes denote the peak value of the normalized cross-correlation function and the number of vanishing ridges from 1 to 5, respectively. The error bars denote the standard deviations of the peak values for 20 kinds of the authentic finite rectangular waves with vanishing ridges having the same number of vanishing ridges. Each curve corresponds to the result for each value of the FRT's order. The symbols of circle in the figure denote the averaged peak values.

We can understand from **Figure 15** that the matching accuracy judged as authentic person becomes worse with increases in the number of vanishing ridges. The matching accuracy, however, becomes better with a decrease in the FRT's order  $p$  except the case of the FT ( $p = 1.0$ ). As the reason, contrary to the case adding random noise shown in **Figure 11**, we can consider that the intensity FRTs with the non-integer orders are not strongly affected by the reduction of the high-spatial frequency components of the authentic fingerprint image by increasing the number of vanishing ridges. However, the probability of rejecting authentic person erroneously is low, because the peak values are nearly 1.0 for every FRT's order and the number of vanishing ridges. This fact means that the FRR would become low.

As shown in **Figures 11** and **15**, the peak values of the normalized cross-correlation functions are nearly fixed at 1.0 when  $p = 1.0$ , however not for other  $ps$ . The reason is, as shown in **Figures 9** and **13**, the intensity FRT for  $p =$

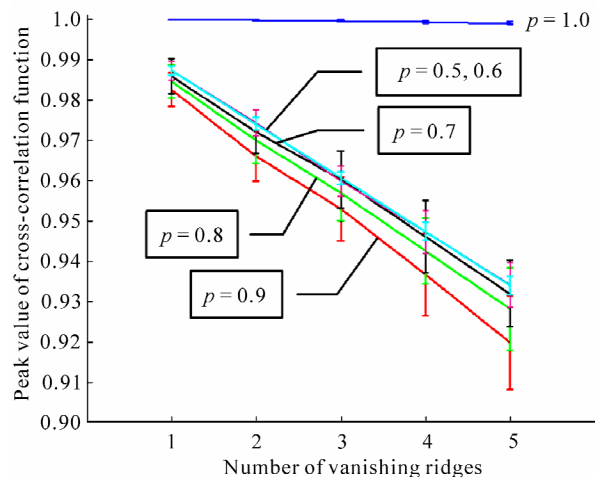


**Figure 15.** Behavior of the peak value of the normalized cross-correlation function between the fingerprint template and the intensity FRT of the authentic finite rectangular waves with vanishing ridges at random positions.

1.0 has a projecting peak and a narrow width and is insensitive to the variations of random noise and vanishing ridges in comparison with those for other  $ps$ .

## 6. Matching Accuracy on the Basis of the MER Derived from the FAR and the FRR

Finally, we determined the matching accuracy by the MER derived from the FAR and the FRR. **Figure 16** indicates the effect of the FRT's order on the peak value of the normalized cross-correlation function between the fingerprint template and the intensity FRT of modified authentic fingerprint image with random noise having various values of the normalized standard deviations. The result for each FRT's order was obtained from that for each FRT's order in **Figure 11**. That is, the error bars denote the standard deviations of the peak values for 100 kinds of authentic finite rectangular waves with random noise having the normalized standard deviation of 0.05 to 0.15 by 0.025, and correspond to the width of spread of the authentic distribution shown in **Figure 3**. The symbols of circle in the figure denote the averaged peak values.

As an example, **Figure 17** is the result showing a set of histograms of the peak value of the normalized cross-correlation function when the FRT's order is 0.9 in **Figures 7** and **16**. In **Figure 17**, the left-side curve is the imposter distribution and the right-side curve is the authentic distribution. The MERs and the authentic thresholds are summarized in **Table 1** for the FRT's order  $ps$  from 1.0 to 0.5 by 0.1. The MER in **Figure 17** is  $1.37 \times 10^{-26}$  and the authentic threshold is 0.992. In **Table 1**, the MERs are very small and the authentic thresholds are

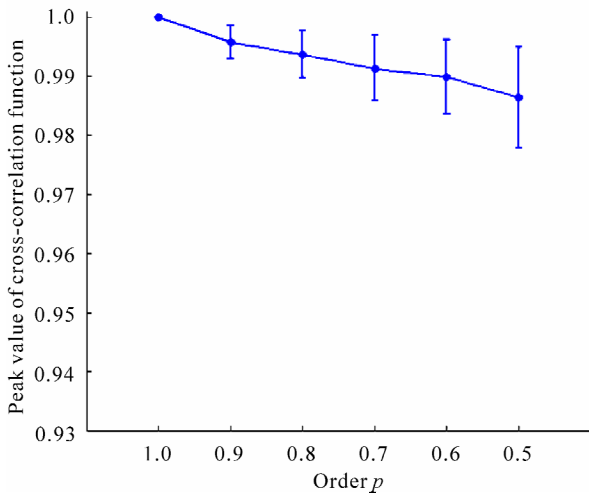


**Figure 16.** Behavior of the peak value of the normalized cross-correlation function between the fingerprint templates and the intensity FRT of the authentic fingerprint images with random noises by changing the FRT's order.

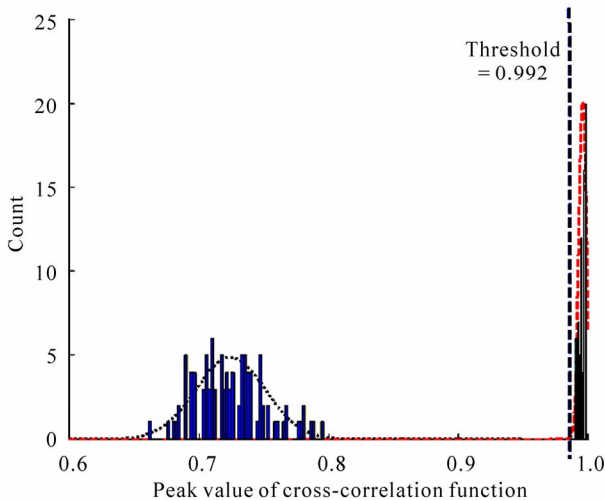


**Figure 17.** A set of histograms corresponding to the impostor and authentic distributions when FRT's order = 0.9 and the random noise is added to the authentic fingerprint image.

**Table 1.** MERs and authentication thresholds for various FRT's orders when considering adding noise.

FRT's order	MER (FAR/FRR)	Threshold
1.0	$2.82 \times 10^{-13}$	0.997
0.9	$1.37 \times 10^{-26}$	0.992
0.8	$3.85 \times 10^{-22}$	0.988
0.7	$8.81 \times 10^{-27}$	0.985
0.6	$2.66 \times 10^{-28}$	0.985
0.5	$3.01 \times 10^{-34}$	0.979

little difference for every FRT's order. Therefore, it is understood that the fingerprint image with dirt can be recognized as an authentic person's one.

Next, **Figure 18** indicates the effect of the FRT's order on the peak value of the normalized cross-correlation function between the fingerprint template and the intensity FRT of the modified authentic fingerprint image with various values of vanishing ridges. The result for each FRT's order was obtained from that for each FRT's order in **Figure 15**. That is, the error bars denote the standard deviations of the peak values for 100 kinds of authentic finite rectangular waves with vanishing ridges from 1 to 5, and correspond to the width of spread of the authentic distribution shown in **Figure 3**. The symbols of circle in the figure denote the averaged peak values.

As an example, **Figure 19** is the result showing a set of histograms of the peak value of the normalized cross-correlation function when the FRT's order is 0.9 in **Figures 7 and 18**. In **Figure 19**, the left-side curve is the impostor distribution and the right-side curve is the authentic distribution. The MERs and the authentic thresholds are summarized in **Table 2** for the FRT's order  $p$ s from 1.0 to 0.5 by 0.1. The MER in **Figure 19** is  $8.46 \times 10^{-7}$  and the authentic threshold is 0.846. In **Table 2**, the MERs are very small and the authentic thresholds are little difference for every FRT's order. Therefore, it is understood that the fingerprint image with vanishing ridges can also be recognized as an authentic person's one.

In particular, the value of MER is the smallest and the best result when the FRT's order is 1.0. However, as

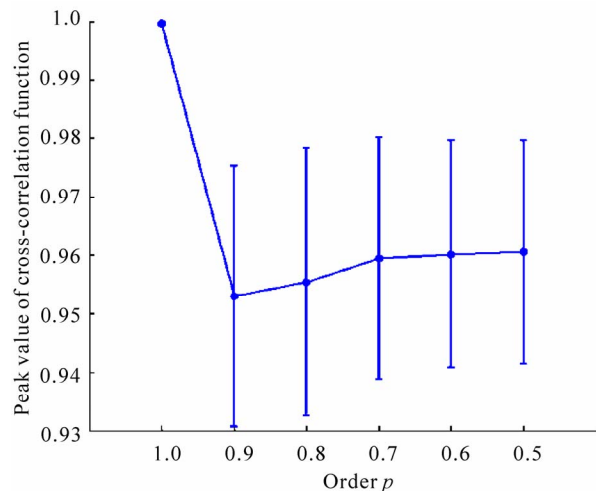


**Figure 18.** Behavior of the peak value of the normalized cross-correlation function between the fingerprint template and the intensity FRT of the authentic fingerprint image with vanishing ridges at random positions by changing the FRT's order.

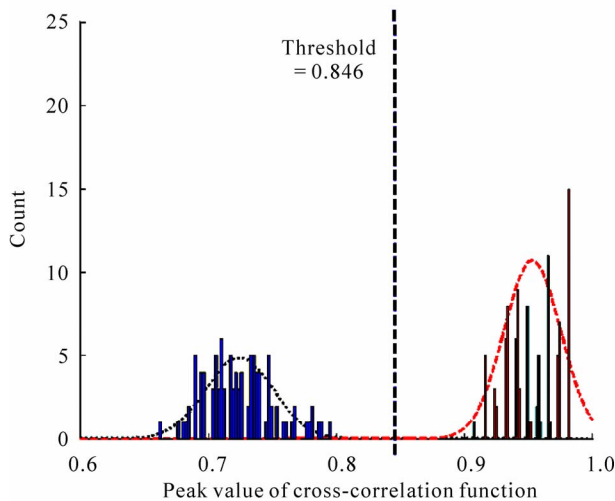


**Figure 19.** A set of histograms corresponding to the impostor and authentic distributions when FRT's order = 0.9 and there exist vanishing ridges at random positions in the authentic fingerprint image.

**Table 2.** MERs and authentication thresholds for various FRT's orders when considering vanishing ridges.

FRT's order	MER (FAR/FRR)	Threshold
1.0	$2.46 \times 10^{-12}$	0.997
0.9	$8.46 \times 10^{-07}$	0.846
0.8	$8.63 \times 10^{-07}$	0.846
0.7	$1.23 \times 10^{-08}$	0.844
0.6	$3.44 \times 10^{-09}$	0.848
0.5	$9.99 \times 10^{-10}$	0.846

already shown in **Table 1**, the value of MER is the biggest and the worst result when the FRT's order is 1.0. Thus, we found that high matching accuracy can be achieved when the FRTs with non-integer values are used. We can also say that the desirable authentic threshold is approximately 0.85 when the matching process is performed by use of the FRT with a non-integer order.

## 7. Conclusions

In this study, we analyzed the matching accuracy of the fingerprint templates generated by our previously proposed data processing method using the FRT. To obtain the MER which is derived from the FAR and the FRR, we used the normalized cross-correlation function between fingerprint template and the intensity FRT of the subject's fingerprint image. First, we generated the fingerprint templates by changing the FRT's order of the authentic finite rectangular wave. Next, we generated

many various impostor finite rectangular waves and derived the intensity FRTs to obtain the FAR. Furthermore, we generated the authentic finite rectangular wave with random noise which is regarded as dirt and the one with vanishing ridges randomly which is regarded as small scar, and derived the intensity FRTs in order to obtain the FRR. As a result, we found that fingerprint templates generated by our data processing method using the FRT can provide high matching accuracy from the viewpoint of the MER.

In the future, we will apply our proposed data processing method using the FRT to real fingerprint images. In the application, the FRT's order is changed randomly in each line of the real fingerprint image. We would make clear the condition of the appropriate range of the FRT's orders in the fingerprint authentication.

## 8. References

- [1] D. Mendlovic and H. M. Ozatkas, "Fractional Fourier Transforms and Their Optical Implementation: I," *Journal of the Optical Society of America A*, Vol. 10, No. 9, 1993, pp. 1875-1881. doi:10.1364/JOSAA.10.001875
- [2] H. M. Ozatkas and D. Mendlovic, "Fractional Fourier Transforms and Their Optical Implementation: II," *Journal of the Optical Society of America A*, Vol. 10, No. 12, 1993, pp. 2522-2531. doi:10.1364/JOSAA.10.002522
- [3] F. J. Marinho and L. M. Bernardo, "Numerical Calculation of Fractional Fourier Transforms with a Single Fast-Fourier-Transform Algorithm," *Journal of the Optical Society of America A*, Vol. 15, No. 8, 1998, pp. 2111-2116. doi:10.1364/JOSAA.15.002111
- [4] H. M. Ozaktas, Z. Zalevsky and M. A. Kutay, "The Fractional Fourier Transform," John Wiley & Sons, Chichester, 2001.
- [5] X. Yang, Q. Tan, X. Wei, Y. Xiang, Y. Yan and G. Jin, "Improved Fast Fractional-Fourier-Transforms Algorithm," *Journal of the Optical Society of America A*, Vol. 21, No. 9, 2004, pp. 1677-1681. doi:10.1364/JOSAA.21.001677
- [6] R. Iwai and H. Yoshimura, "A New Method for Improving Robustness of Registered Fingerprint Data Using the Fractional Fourier Transform," *International Journal of Communications, Network and System Sciences*, Vol. 3, No. 9, 2010, pp. 722-729. doi:10.4236/ijcns.2010.39096
- [7] D. Maltoni, D. Maio, A. K. Jain and S. Prabhakar, "Handbook of Fingerprint Recognition," Springer, New York, 2003.
- [8] H. M. Ozaktas, O. Arikan and M. A. Kutay, "Digital Computation of the Fractional Fourier Transform," *IEEE Transactions on Signal Processing*, Vol. 44, No. 9, 1996, pp. 2141-2150. doi:10.1109/78.536672
- [9] A. Bultheel and H. E. M. Sulbaran, "Computation of the Fractional Fourier Transform," *Applied Computational Harmonic Analysis*, Vol. 16, No. 3, 2004, pp. 182-202. doi:10.1016/j.acha.2004.02.001